# NJC

Accepted Manuscript


This is an *Accepted Manuscript*, which has been through the Royal Society of Chemistry peer review process and has been accepted for publication.

*Accepted Manuscripts* are published online shortly after acceptance, before technical editing, formatting and proof reading. Using this free service, authors can make their results available to the community, in citable form, before we publish the edited article. We will replace this *Accepted Manuscript* with the edited and formatted *Advance Article* as soon as it is available.

You can find more information about *Accepted Manuscripts* in the Information for Authors.

Please note that technical editing may introduce minor changes to the text and/or graphics, which may alter content. The journal's standard Terms & Conditions and the Ethical guidelines still apply. In no event shall the Royal Society of Chemistry be held responsible for any errors or omissions in this *Accepted Manuscript* or any consequences arising from the use of any information it contains.

ROYAL SOCIETY OF CHEMISTRY

www.rsc.org/njc

Cite this: DOI: 10.1039/c0xx00000x

www.rsc.org/xxxxxx

PAPER

# Synthesis of heteroleptic terpyridyl complexes of Fe(II), Ru(II): Optical and electrochemical studies†

**Prakash Chandra Mondal[*a,b], Arun Kumar Manna[c]**

***Received (in XXX, XXX) XthXXXXXXXXX 20XX, Accepted Xth XXXXXXXXX 20XX***

**DOI: 10.1039/b000000x00.**

We report synthesis and characterization of heteroleptic terpyridyl complexes of $d^6$ transition metal ions with $Fe^{2+}$, $Ru^{2+}$ (**1-3**). Furthermore, we study the effect of substitution either electron donating group ($-NH_2$) or electron withdrawing group ($-NO_2$) at the 4'-position in the ligands by means of UV-vis and cyclic voltammetry, and differential pulse voltammetry measurements. Experimentally observed photophysical characteristics of the transition-metal based terypyridyl complexes are explained and supported by quantum chemical calculations in details.

## Introduction

With the discovery of coordination complexes by Alfred Werner, who in 1913 was awarded the Nobel Prize, since then transition metal complexes have found their relevance both in academia and industry, thereby bringing them on common fundamental standpoint. In this context, polypyridyl complexes, which exhibit robust and tuneable photophysical,[1] electrochemical properties[2] and find applications in areas ranging from molecular electronics,[3] catalyst,[4] sensors,[5] drug delivery,[6] and photosensitizers for dye-sensitized solar cells (DSSCs)[7] and to name a few, have become the focal point in extending this relevance. Of all the polypyridyl complexes extensively studied, the 2,2':6',2"-terpyridyl and its derivatives offer several synthetic and structural advantages owing to their excellent structure-properties correlations. This is linked to their achiral nature and higher symmetry ($D_{2d}$) which affords suitability for constructing linear arrays.[8] For instance, the octahedral terpyridyl complexes with free pendant groups are considered as ideal molecular building blocks for the construction of rod like isomer-free networks.[9] Current research interest in the coordination as well as supramolecular chemistry of 2,2':6',2"-terpyridyl derivatives increases enormously after first report on synthesis of terpyridyls by Morgan *et al* back in 1931.[10] The divergent arrangements of donors of the terpyridyls allow the assembly of 1D, 2D or 3D networks. In recent years, Balzani *et al*., Schubert *et al*., Constable *et al*. and others have developed several strategies to synthesize the terpyridyls derivatives and its complexes with transition metal ions mainly for bulk studies.[11] Indeed, redox-active terpyridyl complexes employed onto different substrates (Au, $SiO_x$) to prepare monolayers, dyads, triads, multilayers and various applications have been investigated by our group,[12] Nishihara *et al*.,[13] Haga *et al*.,[14] and others.[15] Functionalized 2,2':6',2"-terpyridyl complexes offer several advantages, to include (i) robustness due to strong metal-to-ligand back bonding [dπ(M)-pπ(L)], (ii) optically rich and redox active, (iii) reversible redox properties which can be tuned either chemically or electro-chemically, and (iv) switchable metal-to-ligand charge-transfer (MLCT) band in the entire visible region.[9,11a] Owing to its synthetic ease, much of the research have been dedicated on homoleptic complexes, in particular with Ru(II), Os(II) centres. Although there are a number of Ir and Ru heteroleptic terpyridyl complexes have been reported but, heteroleptic systems, with Fe(II) are virtually unexplored.[16] Of the same triad, iron complexes have so many advantages, thanks to its abundance and low toxicity over ruthenium and osmium complexes. In this report, we synthesize heteroleptic terpyridyl complexes of Fe(II), Ru(II) and make an attempt to study their optical and electrochemical properties. The heteroleptic complexes have been characterized by complementary analysis techniques such as NMR, mass spectra, FTIR and their optical and electrochemical measurements. Detailed computational study was performed to calculate energy band gap between highest occupied molecular orbital (HOMO) and lowest unoccupied molecular orbital (LUMO).

## Experimental sections

**Preparation of complexes (1-3).** Preparation and characterization data of the ligands are given in Supporting Information (Scheme S1-S3, Fig. S1-S4).

**Complex 1.** A solution of 4'-pyridyl terpyridyl (4'-pytpy) (31 mg, 0.1 mmol) in hot ethanol (8 mL) was added a solution of $FeCl_2$ (12.6 mg, 0.1 mmol) in ethanol (10 mL) and the reaction mixture was stirred for 10 min. 4'-phenyl-terpyridiyl (4'-phtpy) (31 mg, 0.1 mmol) in ethanol was added drop wise with constant stirring. Subsequently the reaction mixture was refluxed under argon for 8 h (Scheme 1). After cooling the reaction mixture, it was filtered to remove any unreacted materials and then $NH_4PF_6$ solution (50 mg in 1 mL ethanol) was added slowly to precipitate out. The content was filtered through celite and washed with ample amount of deionized water and diethyl ether. The solid product obtained was recrystallized with acetonitrile-acetone (1:2, v/v) to get the micro-crystalline solid. $^1$H NMR ($CD_3CN$) δ/ppm: 9.22 (d, 2H, $J$ = 3.37 Hz, $H^{3'}$), 9.19 (d, 2H, $J$ = 3.82 Hz, $H^{3'a}$), 9.02 (m, 2H, $J$ = 7.5 Hz, $H^m$), 8.62 (m, 4H, $H^3$+$H^{3a}$), 8.32

(d, 2H, $J$ = 8.2 Hz, $H^{o}$), 8.23 (t, 2H, $J$ = 7.6 Hz, $H^{ma}$), 7.94 (m, 4H, $H^{4}$+$H^{4a}$), 7.81 (t, 2H, $J$ = 7.86 Hz, $H^{oa}$), 7.73 (m, 1H, $H^{p}$), 7.19 (dt, 4H, $J$ = 7.8, 4.6 & 1.6 Hz, $H^{6}$+$H^{6a}$), 7.09 (dt, 4H, $J$ = 7.2, 5.0 and 1.8 Hz, $H^{5}$+$H^{5a}$). UV-vis ($CH_3CN$) $\lambda_{max}$/nm ($\varepsilon/10^3$ $dm^3$ $mol^{-1}$ $cm^{-1}$): 567 (25.9). FTIR (KBr): 1608 (w), 1410 (w), 838 (vs) $cm^{-1}$.

**Complex 2.** A solution of 4'-aminophenyl terpyridyl (4'-$NH_2$phtpy) (65 mg, 0.20 mmol) was added dropwise to the solution of $FeCl_2$ (26 mg, 0.20 mmol, in 15 mL ethanol) at room temperature with constant stirring in 30 min span time. Subsequently, 4'-nitrophenyl terpyridyl (4'-$NO_2$phtpy) (71 mg, 0.20 mmol, in 15 mL hot ethanol) in 15 mL hot ethanol was added drop-wise to the reaction mixture (Scheme 1). The reaction mixture was refluxed overnight under constant stirring at 75°C. After cooling to room temperature, the mixture was filtered to remove the unreacted materials and then aqueous solution of $NH_4PF_6$ (50 mg in 5 mL distilled water) was added slowly to the filtrate. A deep purple colour precipitate was obtained which was filtered and washed with ample of water, ethanol and diethyl ether, and recrystallized in a mixture of acetonitrile-toluene (1:1, v/v). $^1$H NMR ($CD_3CN$) δ/ppm: 9.21 (s, 2H, $H^{3'a}$), 9.01 (d, 4H, $J$ = 8.64 Hz, $H^{3'}$+$H^{ma}$), 8.63 (m, 4H, $H^{3a}$+$H^{oa}$), 8.50 (t, 2H, $J$ = 8.5 Hz, $H^{4a}$), 8.12 (dd, 2H, $J$ = 6.4 Hz, $H^{5a}$), 7.90 (m, 4H, $H^{o}$+$H^{3}$), 7.18 (m, 4H, $H^{6a}$+$H^{m}$), 7.09 (m, 4H, Hz, $H^{4}$+$H^{6}$), 6.99 (dd, 2H, $J$ = 8.26 Hz, $H^{5}$), 4.83 (s, 2H,-$NH_2$). UV-vis ($CH_3CN$) $\lambda_{max}$/nm ($\varepsilon/10^3$ $dm^3$ $mol^{-1}$ $cm^{-1}$): 579 (33.30), ESI-MS: m/z: 367 $[M-2PF_6]^{2+}$. FTIR (KBr): 3402 (w), 1600 (m), 1346 (w), 840 (vs), 558 (m) $cm^{-1}$.

**Complex 3**: Preparation of **3** was carried out in two steps: (i) synthesis of Ru(pytpy)$Cl_3$[17] followed by reaction with 4'-aminophenyl terpyridyl in equimolar ratio. In brief, a suspension of $RuCl_3.3H_2O$ (78 mg, 0.323 mmol) and 4'-pyridyl-terpyridyl (100 mg, 0.323 mmol) in 20 mL ethanol was refluxed for 6 h. A dark brown precipitate was formed which was filtered and washed with plenty of water followed by diethyl ether and then dried in vacuum to yield Ru(pytpy)$Cl_3$. (ii) Ru(pytpy)$Cl_3.3H_2O$ (54.8 mg, 0.1 mmol) and 4'-aminophenyl terpyridine (4'-$NH_2$phtpy) (33 mg, 0.1 mmol) were suspended in 20 mL ethylene glycol then 2-3 drops of N-ethyl morpholine were added and the reaction mixture was refluxed for 24 h under argon at 150°C with constant stirring and with exclusion of light (Scheme 1). The resulting red solution was cooled to room temperature and treated with $NH_4PF_6$ solution (50 mg in 1 mL ethanol) and the precipitate was allowed to settle. The product was collected over celite, washed with plenty of deionized water and subsequently with diethyl ether. Thereafter, it was dried under vacuum which purified by silica column chromatography using acetonitrile and toluene (1:1, v/v) as eluent. Recrystallization from a solvent mixture of acetonitrile and acetone gives red microcrystalline solid. $^1$H NMR ($CD_3CN$) δ/ppm: 9.01 (s, 4H, $H^{3'a}$+$H^{3'}$), 8.62 (m, 4H, $H^{3a}$+$H^{ma}$), 8.19 (d, 2H, $J$ = 7.8 Hz, $H^{oa}$), 7.92 (m, 4H, $H^{o}$+$H^{3}$), 7.74 (t, 2H, $J$ = 7.8 Hz, $H^{4a}$), 7.67 (m, 2H, $H^{5a}$), 7.58 (m, 2H, $H^{5}$), 7.4 (m, 4H, $H^{4}$+$H^{6a}$), 7.14 (m, 4H, $H^{6}$+$H^{m}$), 5.41 (br, s, 2H, -$NH_2$). UV-vis ($CH_3CN$) $\lambda_{max}$/nm ($\varepsilon/10^3$ $dm^3$ $mol^{-1}$ $cm^{-1}$): 501 (39.18), ESI-MS: m/z: 368 $[M-2PF_6]^{2+}$. FTIR (KBr): 3402 (w), 1600 (vs), 1410 (m), 788 (m) $cm^{-1}$.

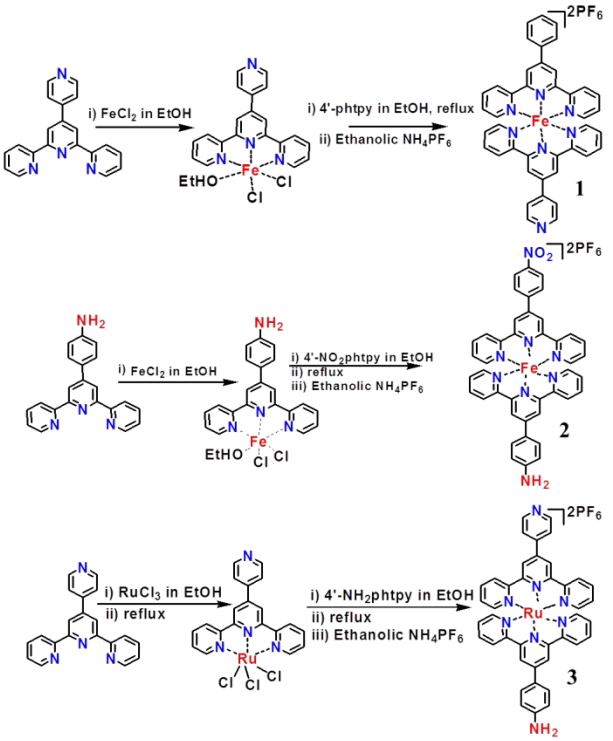


**Scheme 1:** Schematic presentation for preparation heteroleptic terpyridyl complexes with Fe(II) (**1** & **2**) and Ru(II) (**3**).

## Results and discussion

**Synthetic procedure.** The terpyridyl derivatives were synthesized according to Kröhnke methodology[18] which relies on condensation of the corresponding aromatic aldehyde with two equivalent of 2-acetyl pyridine in the presence of strong base such as $^t$BuOK in anhydrous THF or NaOH/KOH in MeOH/EtOH. The intermediate, 1,5-diketone obtained is then reacted with liq. $NH_3$ or solid $NH_4OAc$ under refluxing conditions to afford desired terpyridyl derivative in yields ranging from 60 to 80%. Plausible mechanism of preparation of terpyridyl derivatives is given in Scheme S4 in Supporting Information. Preparation of heteroleptic complexes follow a simple procedure where the appropriate metal salt, such as $RuCl_3.3H_2O$, or $FeCl_2$ was reacted with 4'-functionalized terpyridine in proper molar ratio. For example, a 1:1 mole ratio of metal salt/ligand followed by the addition of second ligand. The exchange of counter anion ($Cl^-$) with hexafluorophosphate ($PF_6^-$) results in precipitation of the desired product. The complexes are light sensitive, therefore, all the process including the reaction, washing, purification, recrystallization, were carried out under dark and the final compounds was stored in desiccator under $N_2$.

The NMR spectra of the complexes show a considerable shift as compared to the free ligands, which firmly indicates strong metal-ligand interactions in the resulting complexes. The more up field shifts of the proton may be traced to more shielding due to the presence of the electron rich metal ions. **1** reveals all expected peaks in its $^1$H NMR spectrum (Fig. 1a). It shows a doublet at δ = 9.22 ppm with $J$ = 3.37 Hz, assigned as $H^{3'}$. The $H^{3'a}$ proton

appears as doublet at δ = 9.19 ppm and the weak magnetic interaction was found at $J$ = 3.82 Hz. On the other hand, the higher δ of $H^{3'}$ than $H^{3'a}$ observed, due to presence of pyridyl group which is a weak electron withdrawing group. The proton, $H^{m}$ appears at δ = 9.02 ppm, show multiplet and $J$ = 7.5 Hz. Both the protons, $H^{3}$ and $H^{3a}$ merge at δ = 8.62 ppm. The expected ortho coupling ($J$ = 8.2 Hz) is observed for $H^{o}$ and appeared at δ = 8.32 ppm as doublet (d). Further, $^{1}$H-$^{1}$H COSY spectra show excellent correlation between neighbouring protons of **1** (see Fig. S5**)**. **2** show a broad peak at δ = 4.83 ppm which assigned as –$NH_2$ peak (Fig. 1b, inset). The $H^{3'a}$ appears as singlet at δ = 9.2 ppm. The two protons, $H^{ma}$+$H^{3'}$ appear at δ = 9.01 ppm, while $H^{3a}$ + $H^{oa}$ appear at δ = 8.63 ppm as multiplet (m). The $H^{4a}$ appear at δ = 8.63 ppm which was splitted by the adjacent protons, as a result it shows multiplet (m), while $H^{m}$ + $H^{5}$ appear as multiplet at δ = 7.09 ppm. The protons $H^{4}$ and $H^{5a}$ show double doublet (dd) and appear at δ = 6.99 and 8.12 ppm, respectively. The other protons $H^{3}$+$H^{6a}$ and $H^{o}$ + $H^{6}$ appear as multiplet at δ = 7.9 and 7.18 ppm, respectively. **3** show a broad peak at δ = 5.42 ppm assigned as –$NH_2$ group and appears as singlet. The peaks at δ = 9.01 ppm is assigned as $H^{3'}$+$H^{3'a}$, whereas $H^{3a}$ + $H^{ma}$ come at δ = 8.62 ppm (see Fig. S6). On the other hand, the proton $H^{oa}$ gives signal at δ = 8.19 ppm as doublet (d) with $J$ = 7.8 Hz. The protons, $H^{o}$+$H^{3}$ show peak at δ = 7.92 ppm (m), while $H^{4a}$, $H^{5a}$ and $H^{5}$ come at δ = 7.74 (at $J$ = 6.8 Hz), 7.67 (m) and 7.58 ppm respectively. The peaks observe at more up field for $H^{4}$+$H^{6a}$ and $H^{6}$+$H^{m}$ and appear at δ = 7.4 and 7.14 ppm respectively. A total number of 30 protons are estimated from the peak integration which is also expected from the molecular structure of **3**.

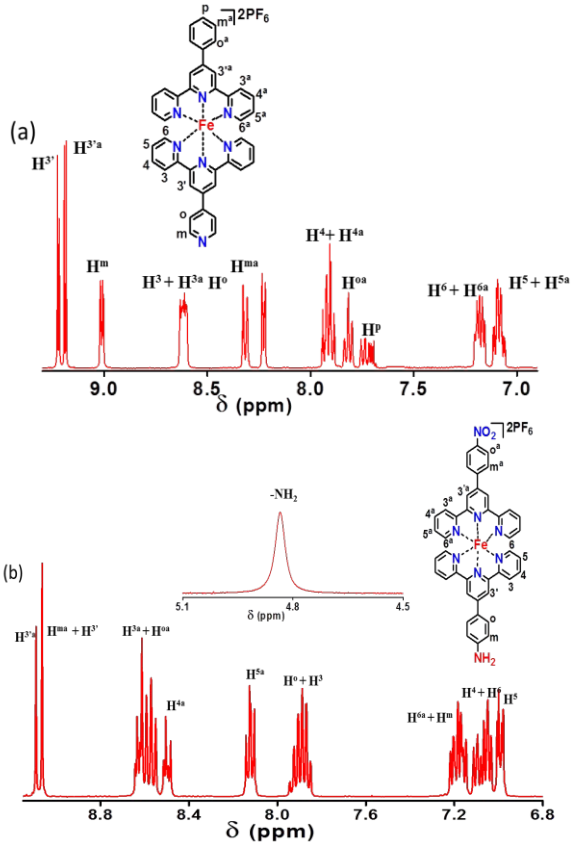


**Fig 1:** Schematic presentation for preparation heteroleptic terpyridyl complexes with Fe(II) (**1** & **2**) and Ru(II) (**3**).

FTIR spectra analysis are made by comparison with those reported for 2,2':6',2"-terpyridyl derivatives.[19] In all cases, a strong stretching frequency is observed in the range of ν = 836-840 $cm^{-1}$, assigned as P-F vibration indicating the presence of $PF6^{-}$ counter anion in the complexes. The stretching frequency for C=C and C=N is observed at higher value for complexes as compared to free terpyridyls. For example, **1** exhibits two moderate peaks at ν = 1608 and 1410 $cm^{-1}$ attributed as C=C and C=N, respectively. In addition, an intense peak observed at ν = 838 $cm^{-1}$ assigned as P-F stretching. **2** shows strong peaks at ν = 1608 and 838 $cm^{-1}$ assigned as C=C and P-F stretching frequency. The compound containing both electron donating group (-$NH_2$) as well as electron withdrawing group (-$NO_2$) i.e., **2** shows stretching frequencies at ν = 3402 and 1346 $cm^{-1}$ which confirms the presence of both -$NH_2$ and -$NO_2$ group in the complex. **3** displays a weak signal at ν = 3402 $cm^{-1}$ ascribed as N-H stretching frequency and a strong frequency at ν = 3402 $cm^{-1}$ assigned as C=C vibration.

**2** exhibits molecular ion peak with maximum intensity and appeared at m/z = 367.09 ascribed as $(M\text{-}2PF_6)^{2+}$ as depicted in Figure S7, while **3** displayed intense molecular ion peak at m/z = 368.08 assigned as $(M\text{-}2PF_6)^{2+}$ (Fig. S8).

**Optical properties.** The terpyridyl based ligands show LC transitions in the range of $\lambda_{max}$ = 278-289 nm and $\lambda_{max}$ = 229-257 nm which are attributed to n ⟹π* and π ⟹ π* transitions, respectively. In addition, strong absorption bands at $\lambda_{max}$ = 310-375 nm also appeared which is assigned as intra-ligand charge-transfer (ILCT) transition. Metal complexes show intense metal-to-ligand charge-transfer (MLCT) transitions in visible region. For example, **1** shows an intense MLCT band at $\lambda_{max}$ = 567 nm (ε = 26,000 $M^{-1}$ $cm^{-1}$) in $CH_3CN$ as (Fig. 2a). A blue shift by 2 nm as compared to Fe(pytpy)$_2$ confirms the formation of heteroleptic compound, since phtpy group is a weak electron donor than pytpy.[20] **2** containing both electron donating (-$NH_2$) and electron withdrawing (-$NO_2$) group displays a red shift by 9 nm nm) with high extinction coefficient (ε = 33,300 $M^{-1}$ $cm^{-1}$) as compared to **1**. The compound exhibits an intense MLCT transition at $\lambda_{max}$ = 576 nm (Fig. 1b). The ligands causes a large destabilisation of the dπ of metal HOMO than the π* (tpy) LUMO, as a result the HOMO-LUMO energy gap decrease and the red shift of MLCT spectra occurs.[21] A similar observations were made with the MLCT band of **3** which exhibits a sharp MLCT transition at $\lambda_{max}$ = 501 nm (ε = 39,200 $M^{-1}$ $cm^{-1}$) (Fig. 1c). In this case, a red shift by 11 nm was observed as compared to the spectrum of homoleptic Ru(pytpy)$_2$.[12d]

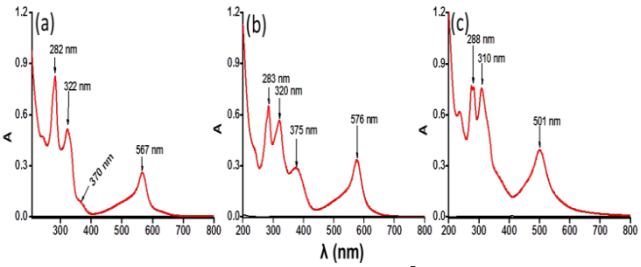


**Fig 2:** UV-Vis spectra in dry $CH_3CN$ ($1 \times 10^{-5}$ M) of (a) **1**, (b) **2**, and (c) **3,** respectively.

**Electrochemical properties.** Electrochemical properties of all the complexes were studied by cyclic voltammetry and differential pulse voltammetry measurements. **1** reveals a single

electron oxidation peak at +1.19 V (vs Ag/AgCl), attributed to the $Fe^{2+/3+}$ couple (Fig. 3a). A cathodic shift of the peak potential ($\Delta E$ = -30 mV) observed in case of **1** as compared to $Fe(pytp)_2$ confirms the formation of heteroleptic compound. The more cathodic shift of the peak potential indicated that phenyl group acts as a weak electron donor.[17] DPV studies exhibits single oxidation process at +1.15 V and reduction peak at +1.13 V which further rules out the possibility of any homoleptic counterpart formation (Fig. 3b). Half-wave redox potential, $E_{1/2}$ was estimated at +1.15 V (vs Ag/AgCl) and it is found to be constant over the scan rate ranging from 100-1000 mV $s^{-1}$ (see Table S1 in the Supporting Information). A linear dependence ($R^2$ = 0.98) of the peak current density as a function of square root of scan rate was observed (Fig. 3c), indicating diffusion controlled process at the molecule-electrode interface. The reversible electrochemical behaviour of the complex was further confirmed from the peak-to-peak separation values, $\Delta E_p$ (70-94 mV) and the plot of ratio of anodic peak current density to cathodic peak current density ($I_{pa}/I_{pc}$) as a function of scan rate, which is almost unit throughout the scan rates (Fig. 3d). The full-width at half-maxima (FWHM) values was found in the range of +160-195 mV, as calculated from the anodic peak current. The higher value arises might be effect of interaction between the electro-active species.[22] **2** reveals two oxidation peaks and single reduction peak in the voltamogramm. The peak at lower potential i.e., +1.03 V vs Ag/AgCl assigned as ligand cantered (-$NH_2$) oxidation, while the peak at higher value i.e., +1.21 V, due to the $Fe^{2+/3+}$ couple (Fig. 4a). An increase of oxidation potential by 20 mV than **1**, confirms the incorporation of 4'-nitrophenyl-terpyridyl into **2**. The electrochemical waves also exhibit a single reduction peak at +1.12 V (vs Ag/AgCl). DPV studies further prove the existence of –$NH_2$ group in the complex.[23]

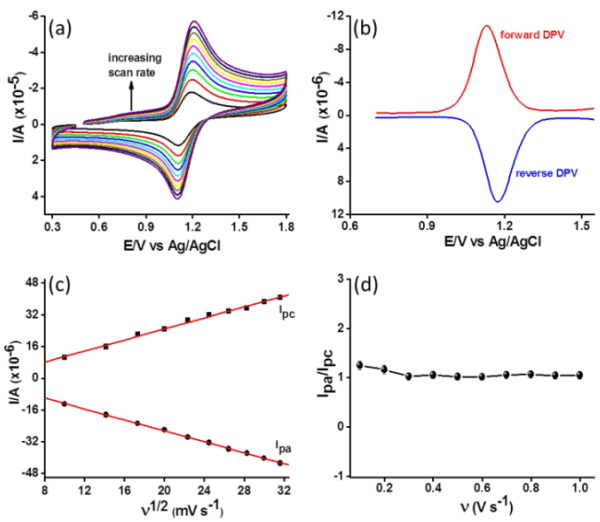


**Fig 3:** Cyclic voltammograms of **1** (1 mM solution, 0.1 M $TBAPF_6$) in dry $CH_3CN$ recorded at 100-1000 mV $s^{-1}$, (b) differential pulse voltammograms, (c) the plots of cathodic and anodic current density as a function of square root of the scan rates ($\nu$), and (d) the plot of the ratio of anodic to cathodic current ($I_{pa}/I_{pc}$) as a function of scan rates.

Remarkably, totally different voltammograms were obtained for **3**. From the shape of the electrochemical waves (see Fig. S9), it is confirmed that the electrochemical phenomenon is diffusionless rather than the diffusion controlled. The cyclic voltammograms show the metal centre based oxidation at +1.41 V (vs Ag/AgCl). Furthermore, it exhibits almost constant $E_{1/2}$ at +1.4 V (vs Ag/AgCl) during the electrochemical measurements. The lower peak-to-peak separation values ($\Delta E_p$ = 10-20 mV) over the scan rates which unequivocally indicates adsorption of the complex on glassy carbon electrode was used as working electrode. In this case the ligand cantered oxidation peak was not observed, that further demonstrates the adsorption of the complex through –$NH_2$ group. Additionally, a linear behaviour ($R^2$ = 0.99) of the cathodic and anodic current density as a function of the scan rates (Fig. S10) unequivocally reveals the attachment of the complex over the glassy carbon electrode.

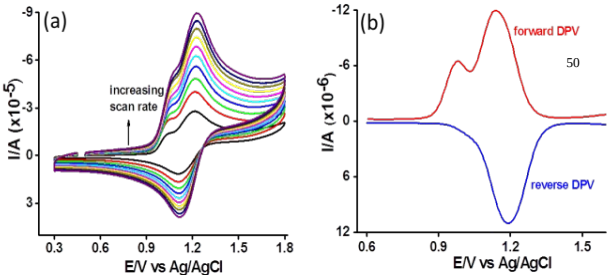


**Fig 4:** (a) Cyclic voltammograms of **2** (1 mM solution, 0.1 M $TBAPF_6$) in dry $CH_3CN$ recorded at 100-1000 mV $s^{-1}$, and (b) differential pulse voltammograms.

## DFT calculations

To gain a microscopic understanding of the observed photophysical properties, we have performed theoretical calculations based on density functional theory (DFT) and time-dependent DFT (TDDFT). Geometries of three metal terpyridyl complexes (1, 2 and 3) in their +2 charged state are fully optimized considering different spin states and without imposing any symmetry constraint by using unrestricted DFT method employing range-separated hybrid exchange and correlation ωB97XD functional that was developed to accounts for long-range charge transfer and dispersion interactions,[24] with 6-31G(d) basis set[25,26] for light elements (H, C, N, O) and LANL2DZ basis set[27] augmented with an effective core potential (ECP) for metal atoms (Fe and Ru). Solvent effects are considered by means of an implicit solvent model, polarizable continuum model (PCM)[28,29] using acetonitrile dielectrics representing polar solvent used in experimental measurements. Normal modes analysis were performed in order to confirm minimum energy structures on the ground state potential energy surface at the same calculation level employed for the geometry optimization. Excited state calculations, solving for 30 low-lying singlet excited states were implemented by using TDDFT method employing 6-31+G(d,p) basis set for light atoms and LANL2DZ for the metals with an ECP for representing core electrons potential. TDDFT calculations were carried out in acetonitrile using the PCM non-equilibrium version[30] at the solvent affected ground state geometry. For the sake of completeness we have also performed excited states calculations by using two other DFT exchange correlation functional: long-range corrected Coulomb attenuated CAM-B3LYP[31] and semi-empirical B3LYP[32] hybrids. All calculations were carried out by using Gaussian 09 DFT software package.[33]

Calculations predict broken symmetry singlet as the minimum

energy spin state for all three complexes. Optimized structures and frontier molecular orbitals (HOMO: highest occupied molecular orbital and LUMO: lowest unoccupied molecular orbital) energies and isosurfaces calculated using ωB97XD functional for three complexes are shown in Fig. 5. It is found from the relaxed structures that two tpy ligands connected via central metal (M = Fe, Ru) are aligned nearly perpendicularly. M-N bonds along the long molecular axis are slightly smaller (0.1 Å) than the other four M-N bonds present in the complexes (see the numbers listed in Figure 5). HOMO-LUMO gaps calculated using ωB97XD functional are 7.61, 6.36 and 6.59 eV, for the complex 1, 2 and 3, respectively. We find nearly similar gap values predicted by CAM-B3LYP functional; whereas B3LYP functional largely underestimates the gaps (see Table S2 in Supporting Information). It is worth to mention that range-separated density functional (ωB97XD and CAM-B3LYP) provide more accurate gaps by mitigating self-interactions errors and restoring missing derivative discontinuity in exchange-correlation potential. Also as shown in Fig. 5, the HOMO and LUMO orbitals are primarily distributed on either tpy groups in the complex, reflecting a charge transfer (CT) character associated with HOMO to LUMO electronic promotion.

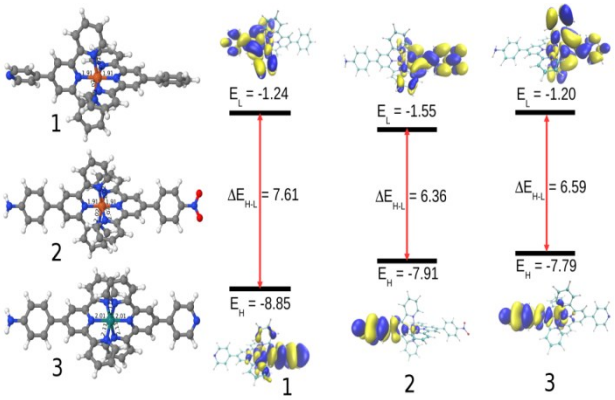


**Fig 5:** Left panel: Structures of three metal (M) complexes optimized in acetonitrile modelled by PCM using DFT method employing ωB97XD functional (important M-N bond lengths are indicated in Å). Right panel: HOMO and LUMO frontier orbitals isosurfaces and their energies and the gap values are depicted. Energies are in eV unit. H and L stand for HOMO and LUMO, respectively.

Next we discuss the optical absorption characteristics of these complexes as calculated by using TDDFT and shown in Fig. 6 and Table S3. We provide a few low-lying excited states energies and associated primary orbitals that are involved in electronic excitations. Calculations show that the first two low-lying excited states found at 470 nm for complex **1** and 475 nm for complex **2** as predicted by ωB97XD functional are associated with vanishing oscillator strengths exhibiting weak ligand-to-metal charge transfer (LMCT) as characterized by the frontier orbitals analysis (see Fig. 6, and Table S3 in the supporting Information). Furthermore, metal-to-ligand charge transfer (MLCT) absorption occurs at around 360 nm, with substantially strong absorption peaks (indicated by large oscillator strength) appeared at 334 and 340 nm, respectively for complex **1** and **2**, and these are characterized as ligand-to-ligand CT (LLCT). On the other hand, the complex **3** only exhibits low-lying MLCT transitions and the first peak appeared at 404 nm. Differences between the calculated and experimentally measured low-lying peak positions are estimated to be about 0.4-0.6 eV. This deviation can be attributed to an anticipated large electrostatic stabilization of CT excited states in the polar environment present by acetonitrile dielectrics, which is not captured quantitatively by the TDDFT method employing non-equilibrium PCM solvation model, as implemented in Gaussian09. We also note that apparently better agreement of the B3LYP prediction with the experimental MLCT energy for the complex **3** is mainly due to a large underestimation of the HOMO-LUMO gap (see Table S2 and Table S3). Our computational results are in general good agreement with the observed experimental photophysical properties.

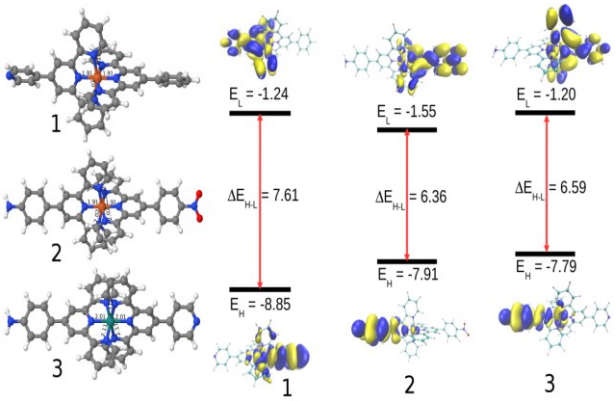


**Fig 6:** Left panel: Structures of three metal (M) complexes optimized in acetonitrile modelled by PCM using DFT method employing wB97XD functional (important M-N bond lengths are indicated in Å). Right panel: HOMO and LUMO frontier orbitals isosurfaces and their energies and the gap values are depicted. Energies are in eV unit. H and L stand for HOMO and LUMO, respectively.

## Conclusions

Heteroleptic complexes of 4'-functionalized terpyridyl with $Fe^{2+}$, $Ru^{2+}$ have been prepared and fully characterized. The electron donating group increased the position of the wavelength of the metal to ligand charge-transfer band and also increased molecular extinction co-efficient. Shifting in wavelength of the metal to ligand charge-transfer bands and redox potentials of the complexes have been observed with variation of functional groups at 4'-position in the terpyridyl ligands. Further, electrochemical deposition of the complexes through -$NH_2$ group has also been detected during the electrochemical study which was further confirmed from the linear behaviour of faradic current with scan rates. Both the DFT and TDDFT calculations provide microscopic understanding of the measured photophysical properties of the complexes investigated.

## Acknowledgements

Financial support from DST-Nano-Mission is highly acknowledged. The authors are highly thankful to the University Sophisticated Instrument Centre (USIC), University of Delhi, India, and SAIF, CDRI, Lucknow, for providing the NMR and ESI Mass spectra facility, respectively. The authors also thank Council of Scientific and Industrial Research, New Delhi for

senior research fellowship. Authors are grateful to Prof. Swapan K Pati, JNCASR, Bangalore for providing computing resources for pursuing theoretical calculations.

## Notes and references

[a]*Department of Chemistry, University of Delhi, Delhi-110007, India E-mail: mondalpc@gmail.com*

[b]*Present address: Department of Chemical Physics, Weizmann Institute of Science, Rehovot-7610001, Israel*

[c]*Department of Materials and Interfaces, Weizmann Institute of Science, Rehovot-7610001, Israel*

†A tribute to late Prof. Tarkeshwar Gupta, University of Delhi.
Electronic Supplementary Information (ESI) available. See DOI: 10.1039/b000000x/

1 (a) J. D. Knoll, B. A. Albani and C. Turro, *Acc. Chem. Res*., 2015, Adv. article; (b) N. Tuccitto, V. Ferri, M. Cavazzini, S. Quici, G. Zhavnerko, A. Licciardello and M. A. Rampi, *Nat. Mat*., 2009, **8**, 41; (c) D. G. Brown, N. Sanguantrakun, B. Schulze, U. S. Schubert and C. P. Berlinguette, *J. Am. Chem. Soc*., 2012, **134**, 12354; (d) D. C. Goldstein, Y. Y. Cheng, T. W. Schmidt, M. Bhadbhade and P. Thordarson, *Dalton Trans*., 2011, **40**, 2053.

2 (a) J. A. Thomas, *Coord. Chem. Rev*., 2013, **257**, 1555; (b) A. Baron, C. Herrero, A. Quaranta, M.-F. Charlot, W. Leibl, B. Vauzeilles and A. Aukauloo, *Chem. Commun*., 2011, **47**, 11011; (c) T. J. Meyer, *Acc. Chem. Res*., 1989, **22**, 163.

3 (a) J. R. Peterson, T. A. Smith and P. Thordarson, *Chem. Commun*., 2007, 1899; (b) J. H. Alstrum, M. K. Brennaman and T. J. Meyer, *Inorg. Chem*., 2005, **44**, 6802; (c) F. Barigelletti and L. Flamigni, *Chem. Soc. Rev*., 2000, **29**, 1; (d) L. C. Sun, L. Hammarström, B. Åkermark and S. Styring, *Chem. Soc. Rev*., 2001, **30**, 36.

4 (a) F. Puntoriero, A. Sartorel, M. Orlandi, G. G. La, S. Serroni, M. Bonchio, F. Scandola and S. Campagna, *Coord. Chem. Rev*., 2011, **255**, 2594; (b) C. J. Kleverlaan, M. T. Indelli, C. A. Bignozzi, L. Pavanin, F. Scandola, G. M. Hasselman and G. J. Meyer, *J. Am. Chem. Soc*., 2000, **122**, 2840; (c) M. Hirahara, S. Nagai, K. Takahashi, K. Saito, T. Yui and M. Yagi, *Inorg. Chem*., 2015, **54**, 7627; (d) V. Singh, P. C. Mondal, M. Chhatwal, Y. L. Jeyachandran and M. Zharnikov, *RSC Adv*., 2014, **4**, 23168.

5 (a) P. C. Mondal, V. Singh and B. Shankar, *New J. Chem*., 2014, **38**, 2679; (b) V. Singh, P. C. Mondal, J. Y. Lakshmanan, M. Zharnikov and T. Gupta, *Analyst*, 2012, **137**, 3216; (c) N. Mourtzis, P. C. Carballada, M. Felici, R. J. M. Nolte, R. M. Williams, L. de Cola and M. C. Feiters, *Phys. Chem. Chem. Phys*., 2011, **13**, 7903; (d) S. Karlsson, J. Boixel, Y. Pellegrin, E. Blart, H. Becker, F. Odobel and L. Hammarstroem, *J. Am. Chem. Soc*., 2010, **132**, 17977.

6 (a) J. A. Thomas, *Chem. Soc. Rev*., 2015, **44**, 4494; (b) S. Stimpson, D. R. Jenkinson, A. Sadler, M. Latham, A. Wragg, A. J. H. M. Meijer and J. A. Thomas, *Angew. Chem., Int. Ed*., 2015**, 54**, 3000; (c) T. Wilson, P. J. Costa, V. Felix, M. P. Williamson and J. A. Thomas, *J. Med. Chem*., 2013, **56**, 8674; (d) V. Singh, P. C. Mondal, A. Kumar, Y. L. Jeyachandran, S. K. Awasthi, R. D. Gupta and M. Zharnikov, *Chem.Commun*., 2014, **50**, 11484; (e) U. Basu, I. Khan, A. Hussain, P. Kondaiah and A. R. Chakravarty, *Angew. Chem., Int. Ed*., 2012, **51**, 1.

7 (a) B. O'Regan and M. Grätzel, *Nature*, 1991, **353**, 737; (b) M. Grätzel, *Acc. Chem. Res*., 2009, **42**, 1788.

8 (a) L. Flamigni, J. P. Collin and J. P. Sauvage, *Acc. Chem. Res*., 2008, **41**, 857; (b) L. Hammarström and O. Johansson, *Coord. Chem. Rev*., 2010, **254**, 2546.

9 E. C. Constable, *Coord. Chem. Rev*., 2008, **252**, 842.

10 S. G. Morgan and F. H. Burstall, *J. Chem. Soc*., 1931, 20.

11 (a) E. C. Constable, *Chem. Soc. Rev*., 2007, **36**, 246; (b) B. Happ, A. Winter, M. D. Hager and U. S. Schubert, *Chem. Soc. Rev*., 2012, **41**, 2222; (c) J. P. Sauvage, J. P. Collin, J. C. Chambron, S. Guillerez, C. Coudret, V. Balzani, F. Barigelletti, L. de Cola and L. Flamigni, *Chem. Rev*., 1994, **94**, 993.

12 (a) P. C. Mondal, *New J. Chem*., 2015, **39**, 7403; (b) P. C. Mondal, J. Y. Lakshmanan, H. Hamoudi, M. Zharnikov and T. Gupta, *J. Phys. Chem. C*, 2011, **115**, 16398; (c) P. C. Mondal, M. Chhatwal, Y. L. Jeyachandran and M. Zharnikov, *J. Phys. Chem. C*, 2014, **118**, 9578; (d) P. C. Mondal, V. Singh, Y. L. Jeyachandran and M. Zharnikov, *ACS Appl. Mat. Interfaces*, 2015, **7**, 8677; (e) A. Kumar, M. Chhatwal, P. C. Mondal, V. Singh, A. K. Singh, D. A. Cristaldi, R. D. Gupta and A. Gulino, *Chem. Commun*., 2014, **50**, 3783; (f) T. Gupta, P. C. Mondal, A. Kumar, J. Y. Lakshmanan and M. Zharnikov, *Adv. Funct. Mater*., 2013, **23**, 4227.

13 (a) Y. Nishimori, K. Kanaizuka, T. Kurita, T. Nagatsu, Y. Segawa, F. Toshimitsu, S. Muratsugu, M. Utsuno, S. Kume, M. Murata and H. Nishihara, *Chem. Asian J*., 2009, **4**, 1361; (b) R. Sakamoto, S. Katagiri, H. Maeda and H. Nishihara, *Coord. Chem. Rev*., 2013, **257**, 1493; (c) K. Takada, R. Sakamoto, S.-T. Yi, S. Katagiri, T. Kambe and H. Nishihara, *J. Am. Chem. Soc*., 2015, **137**, 4681; (d) R. Sakamoto, K.-H. Wu, R. Matsuoka, H. Maeda and H. Nishihara, *Chem. Soc. Rev*., 2015, **44**, 7698.

14 (a) M. Haga, T. Takasugi, A. Tomie, M. Ishizuya, T. Yamada, M. D. Hossain and M. Inoue, *Dalton Trans.*, 2003, 2069; (b) K.-I. Terada, H. Nakamura, K. Kanaizuka, M. Haga, Y. Asai and T. Ishida, *ACS Nano*, 2012, **6**, 1988; (c) K.-I. Terada, K. Kanaizuka, V. M. Iyer, M. Sannodo, S. Saito, K. Kobayashi and M. Haga, *Angew. Chem., Int. Ed*., 2011, **50**, 6287.

15 (a) S. Liatard, J. Chauvin, D. Jouvenot, F. Loiseau and A. Deronzier, *J. Phy. Chem. C*, 2013, **117**, 20431; (b) G. Tsekouras, O. Johansson and R. Lomoth, *Chem. Commun*., 2009, **23**, 3425; (c) J. P. Santos, M. E. D. Zaniquelli, C. Batalini and W. F. de Giovani, *J. Phy. Chem. B*, 2001, **105**, 1780.

16 (a) S. Baitalik, X.-Y. Wang and R. H. Schmehl, *J. Am. Chem. Soc*., 2004, **126**, 16304; (b) D. Maity, S. Mardanya, S. Karmakar and S. Baitalik, *Dalton Trans*., 2015, **44**, 10048; (c) T. Duchanois, T. Etienne, M. Beley, X. Assfeld, E. A. Perpète, A. Monari and P. C. Gros, *Eur. J. Inorg. Chem*., 2014, 3747; (d) D. C. Goldstein, J. R. Peterson, Y. Y. Cheng, R. G. C. Clady, T. W. Schmidt and P. Thordarson, *Molecules*, 2013, **18**, 8959; (e) J. R. Peterson, T. A. Smith and P. Thordarson, *Org. Biomol. Chem*., 2010, **8**, 151; (f) D. Hvasanov, A. F. Mason, D. C. Goldstein, B. Bhadbhade and P. Thordarson, *Org. Biomol. Chem*., 2013, **11**, 4602.

17 E. C. Constable and M. W. C. Thompsona, *J. Chem. Soc., Dalton Trans*., 1994, 1409.

18 F. Kröhnke, *Synthesis*, 1976, 1.

19 C. Postmus, J. R. Ferraro and W. Wozniak, *Inorg. Chem*., 1967, **6**, 2030.

20 G. D. Storrier and S. B. Colbran, *Inorg. Chim. Acta*, 1999, **284**, 76.

21 E. A. Medlycott and G. S. Hanan, *Chem. Soc. Rev*., 2005, **34**, 133.

22 A. J. Bard and L. R. Faulkner, *Electrochemical Methods: Fundamentals and Applications*, 2nd Ed.; John Wiley & Sons: New York, 2001.

23 T. Ohsaka, Y. Ohnuki, N. Oyama, G. Katagiri and K. Kamisako, *J. Electroanal. Chem. Interfacial Electrochem*,. 1984, **161**, 399.

24 J.-D. Chai and M. Head-Gordon, *Phys. Chem. Chem. Phys*., 2008, **10**, 6615.

25 V. A. Rassolov, M. A. Ratner, J. A. Pople, P. C. Redfern and L. A. Curtiss, *J. Comput. Chem*., 2001, **22**, 976.

26 V. A. Rassolov, J. A. Pople, M. A. Ratner and T. L. Windus, *J. Chem. Phys*., 1998, **109**, 1223.

27 P. J. Hay and W. R. Wadt, *J. Chem. Phys*., 1985, **82**, 299.

28 S. Mierts˘, E. Scrocco and J. Tomasi, *Chem. Phys.*, 1981, **55**, 117.

29 M. Cossi, V. Barone, R. Cammi and J. Tomasi, *Chem. Phys. Lett*., 1996, **255**, 327.

30 M. Cossi and V. Barone, *J. Chem. Phys*., 2001, **115**, 4708.

31 R. Kobayashi and R. D. Amos, *Chem. Phys. Lett*., 2006, **420**, 106.

32 A. D. Becke, *J. Chem. Phys*., 1993, **98**, 5648.

33 Gaussian 09, Revision D.01, M. J. Frisch, G. W. Trucks, H. B. Schlegel, G. E. Scuseria, M. A. Robb, J. R. Cheeseman, G. Scalmani, V. Barone, B. Mennucci, G. A. Petersson, H. Nakatsuji, M. Caricato, X. Li, H. P. Hratchian, A. F. Izmaylov, J. Bloino, G. Zheng, J. L. Sonnenberg, M. Hada, M. Ehara, K. Toyota, R. Fukuda, J. Hasegawa, M. Ishida, T. Nakajima, Y. Honda, O. Kitao, H. Nakai, T. Vreven, J. A. Montgomery, Jr., J. E. Peralta, F. Ogliaro, M. Bearpark, J. J. Heyd, E. Brothers, K. N. Kudin, V. N. Staroverov, R. Kobayashi, J. Normand, K. Raghavachari, A. Rendell, J. C. Burant, S. S. Iyengar, J. Tomasi, M. Cossi, N. Rega, J. M. Millam, M. Klene, J. E. Knox, J. B. Cross, V. Bakken, C. Adamo, J. Jaramillo, R. Gomperts, R. E. Stratmann, O. Yazyev, A. J. Austin, R. Cammi, C. Pomelli, J. W. Ochterski, R. L. Martin, K. Morokuma, V. G. Zakrzewski, G. A. Voth, P. Salvador, J. J. Dannenberg, S. Dapprich, A. D. Daniels, Ö. Farkas, J. B. Foresman, J. V. Ortiz, J. Cioslowski, and D. J. Fox, Gaussian, Inc., Wallingford CT, 2009.

# *Table of Content*

## Synthesis of heteroleptic terpyridyl complexes of Fe(II), Ru(II): Optical and electrochemical Studies

Heteroleptic terpyridyl complexes of Fe(II), Ru(II) are synthesized, characterized by complimentary techniques along with optical and electrochemical properties and computational studies.